Critical behaviour of nonequilibrium three-state systems

1993 J. Phys. A: Math. Gen. 26 1559

(http://iopscience.iop.org/0305-4470/26/7/015)

J. Phys. A: Math. Gen. 26 (1993) 1559–1570. Printed in the UK

Critical behaviour of non-equilibrium three-state systems

M C Marques

Departamento de Física da Universidade do Porto, Praça Gomes Teixeira, 4000 Porto, Portugal

Received 7 August 1992, in final form 5 January 1993

Abstract. The phase diagram of two different non-equilibrium three-state systems is here studied by means of MFRG and computer simulations; critical exponents are obtained by a finite-size scaling analysis of the MC data. A symmetry argument used by Grinstein *et al* to predict the critical behaviour of two-state non-equilibrium systems (with up-down symmetry) is shown to apply to these three-state systems (with symmetry of interchange between two of those states).

1. Introduction

The study of phase transitions between steady states of non-equilibrium systems has become a topic of increasing interest extending from physics into other fields [1, 2]. Non-equilibrium critical points have some characteristics in common with equilibrium critical phenomena and it is therefore natural to describe the former using the framework and the techniques developed over recent decades for the latter. However, non-equilibrium phenomena present much greater complexity and one of the difficulties is that its study has to be based on the dynamic rules whereas in equilibrium systems the transition probabilities satisfy detailed balance with respect to a Hamiltonian. Formal analytic results like the existence, in some cases, of an effective Hamiltonian are difficult to derive [3]. For example, the establishment of universality classes cannot be rigorously argued in terms of Gibbs measures flowing, at criticality, towards the same fixed points; however, all the evidence from simulation studies, series expansions, etc [4,5] is that all the non-equilibrium systems studied so far fall into a very small number of universality classes.

The simplest examples of non-equilibrium critical systems and the first to be studied are lattice models where a binary variable is associated with each site. In some of these models the dynamic local rules for the evolution of the site variable allow for the existence of an absorbing state; examples of these are the contact process, the A model, and variations of these (which have been used to describe processes of adsorption–desorption of particles, spreading of a liquid through a porous medium and even propagation of epidemics); they all belong to the universality class of directed percolation. To a different group of two-state non-equilibrium systems belong certain Ising-like models where the non-equilibrium condition arises due to the competition of two (or more) dynamics at different temperatures [5–8]. Results available on these only confirm the argument of Grinstein *et al* [9] according to which the existence of up–down symmetry in two-state dynamic systems implies the same critical behaviour of the equilibrium Ising model.

0305-4470/93/071559+12$07.50

There is considerably less work on non-equilibrium systems with more than two states per site. Perhaps the most thoroughly investigated is again a surface reaction process, the so-called Ziff model [10]; its phase diagram displays a second-order phase transition to an absorbing state and the critical behaviour is one of directed percolation, as predicted by theory when just one absorbing state is present. Among other situations of interest where more than two states per site have to be considered [11], one can also mention a competing two-species directed percolation model [12] where the interplay between the two species results in a complicated phase diagram, but with critical exponents still falling within the universality class of conventional directed percolation.

In the same way that models for adsorption–desorption of particles can be generalized to situations where two or more species are present, one must also investigate the effects of competing dynamics in systems with two or more states per site, thus generalizing the work previously done on non-equilibrium Ising models. The question about the critical behaviour to be expected in these systems is pertinent since the investigation of Grinstein *et al* is addressed to the case of two-state systems. The phase diagram of the one-dimensional BEG model with competing dynamics is being investigated by Mendes *et al* [13] and there seems to be evidence of a different class of universality.

In this work we consider two different non-equilibrium three-state systems, in two dimensions. In both there is competition between two dynamic processes that differ in the way that they treat one among the three available states, but are symmetric in the interchange of the other two states.

The paper is organized as follows. In section 2 we describe the dynamic rules for both systems. In section 3 we present the phase diagrams as obtained by mean-field renormalization group (MFRG), a method which improves on mean-field approaches and has successfully been applied to non-equilibrium critical systems [7,8,14]. In section 4 we present results of numerical simulations, both for the phase diagrams and for the critical behaviour at a few chosen transition points. In section 5 we conclude with a brief discussion of the results.

2. The models

2.1. Model 1: Ising-like model with an average number of mobile vacancies

We consider a square lattice in which the site variable S_i takes the values 1, 0 and -1. The rates for this process are

$$w(S_i \to S_i') = p(S_i')^2 \tfrac{1}{2}[1 + S_i' \tanh x_i] + (1-p)(1 - S_i'^2)$$

with $x_i = J/k_B T \sum_j S_j$. This can be seen as the competition of two processes: with probability p (process A), the state of a randomly chosen site becomes either 1 or -1, the rates being the same as for an Ising Glauber-like process at temperature T; and with probability $1-p$ (process B), the state of that site becomes 0. Process A obeys detailed balance with respect to the Blume–Capel Hamiltonian: $\mathcal{H} = -J\sum_{\langle i,j\rangle} S_i S_j - h\sum_i \delta_{S_i^2,1}$ in the limit that h, the field that couples to the non-ordering parameter $1 - \langle S_i^2\rangle$, becomes infinite; process B does not obey detailed balance with respect to the same Hamiltonian. So for $p \neq 1$, we have, in principle, a non-equilibrium situation. This model describes a system of Ising spins

with an average fraction $1-p$ of vacancies; these vacancies move from site to site, independently of the state of neighbouring sites. This is different from a site annealed diluted Ising model where vacancies move according to rules that relate to a certain Gibbs measure at a given temperature.

2.2. Model 2: Competing Ising and three-state Potts dynamic processes

Again a square lattice is considered and one associates a variable σ_i which can take values 1, 2 or 3 with each site. This non-equilibrium model results from competition between two sets of rules: with probability p the state of a randomly chosen site changes according to a process (C) that obeys detailed balance with respect to the three-state Potts Hamiltonian; and with probability $1-p$ (process D) the state of the chosen site changes necessarily to either two or three, the rates for changes between those two states being the ones for a Glauber Ising process at the same temperature. The evolution rules for this model can then be written:

$$W(\sigma_i \to \sigma_i') = pW_{\text{Potts}} + (1-p)[\delta_{\sigma_i,1}(\tfrac{1}{2}\delta_{\sigma_i',2} + \tfrac{1}{2}\delta_{\sigma_i',3}) + (1-\delta_{\sigma_i,1})W_{\text{Ising}}]$$

where W_{Potts} and W_{Ising} are, respectively, the rates for the Glauber-like dynamics associated with the three- and two-state Potts Hamiltonians. Varying p can, therefore, be seen as a way of varying the asymmetry in the space of Potts states.

3. MFRG analysis

3.1. Model 1

Following closely the approach used before [7, 8] in the study of non-equilibrium Ising models, we start by considering a one-site cluster, and denote by $P(i)$ the probability of its being in state i, given that its neighbours have a probability Q' of being in state 0 and a probability $(1-Q')(1\pm m')/2$ of being in state ± 1. According to section 2.1 the rate at which this one-site cluster changes, for example, from state 0 to state 1, is

$$\begin{aligned} w(0\to 1) = p\Bigg[& R^4(1+m')^4 \frac{e^{4K'}}{e^{4K'}+e^{-4K'}} \\ & + 4R^3(1+m')^3\left(Q'\frac{e^{3K'}}{e^{3K'}+e^{-3K'}} + R(1-m')\frac{e^{2K'}}{e^{2K'}+e^{-2K'}}\right) \\ & + 6R^2(1+m')^2\left(Q'^2\frac{e^{2K'}}{e^{2K'}+e^{-2K'}} + 2Q'R(1-m')\frac{e^{K'}}{e^{K'}+e^{-K'}}\right. \\ & \left. + \frac{1}{2}R^2(1-m')^2\right) + 4R(1+m')\left(Q'^3\frac{e^{K'}}{e^{K'}+e^{-K'}}\right. \\ & + 3Q'R^2(1-m')^2\frac{e^{-K'}}{e^{K'}+e^{-K'}} + \frac{3}{2}Q'^2R(1-m') \\ & \left. + R^3(1-m')^3\frac{e^{-2K'}}{e^{2K'}+e^{-2K'}}\right) + \frac{1}{2}Q'^4 + 4Q'^3R(1-m')\frac{e^{-K'}}{e^{K'}+e^{-K'}} \end{aligned}$$

$$+ 6Q'^2R^2(1-m')^2\frac{e^{-2K'}}{e^{2K'}+e^{-2K'}} + 4Q'R^3(1-m')^3\frac{e^{-3K'}}{e^{3K'}+e^{-3K'}}$$
$$+ R^4(1-m')^4\frac{e^{-4K'}}{e^{4K'}+e^{-4K'}}\Bigg]$$
$$= p\left[\frac{1}{2} + Bm'\right] + O(m'^2)$$

where

$$R = \frac{1-Q'}{2}$$

$$B = 4R^4\frac{e^{4K'}-e^{-4K'}}{e^{4K'}+e^{-4K'}} + 12R^3Q'\frac{e^{3K'}-e^{-3K'}}{e^{3K'}+e^{-3K'}}$$
$$+ (8R^4 + 12R^2Q'^2)\frac{e^{2K'}-e^{-2K'}}{e^{2K'}+e^{-2K'}} + (12R^3Q' + 4RQ'^3)\frac{e^{K'}-e^{-K'}}{e^{K'}+e^{-K'}}.$$

The other rates are easily obtained in a similar way. The time evolution of $P(1)$ and $P(-1)$ is then

$$\begin{aligned}\frac{dP(1)}{dt} &= pP(0)\left[\tfrac{1}{2} + Bm'\right] + pP(-1)\left[\tfrac{1}{2} + Bm'\right] \\ &\quad - P(1)\left[q + p\left[\tfrac{1}{2} - Bm'\right]\right] + O(m'^2) \\ \frac{dP(-1)}{dt} &= pP(0)\left[\tfrac{1}{2} - Bm'\right] + pP(1)\left[\tfrac{1}{2} - Bm'\right] \\ &\quad - P(-1)\left[q + p\left[\tfrac{1}{2} + Bm'\right]\right] + O(m'^2).\end{aligned} \tag{1}$$

In the vicinity of a second-order phase transition, m' is a small quantity; expanding in m', one obtains, from (1), the stationarity condition

$$P(1) - P(-1) = 2pBm'.$$

A similar procedure can be followed for a two-site cluster, considering that neighbours outside the cluster have a probability Q of being in state 0 and probability $(1-Q)(1\pm m)/2$ of being in state ± 1. One starts with the equations that give the time evolution of $P(ij)$, the probability of sites 1,2 being respectively in states i, j. After some algebra, one arrives at the stationarity value for $\mathcal{P}_{II} = P(11) - P(-1-1) + \frac{1}{2}(P(10) - P(-10)) + \frac{1}{2}(P(01) - P(0-1))$:

$$\mathcal{P}_{II} = Cm + O(m^2)$$

where C is a complicated function of p and K. The basic assumption of MFRG is to consider that $\mathcal{P}_I = P(1) - P(-1)$ and $\mathcal{P}_{II}$ must, close to the transition, scale like m' and m. This leads to a RG recursion relation and its fixed point equation:

$$2pBK_c = C(p, K_c). \tag{2}$$

In figure 1, a plot is shown of the p dependence on T_c, as obtained from (2). This MFRG calculation predicts the disappearance of the ferromagnetic phase for a

concentration of vacancies $1 - p$ above a certain value $q^* = 0.571$. This is to be expected since a high concentration of vacancies prevents the propagation of order among the occupied sites. This resembles the Ising model with quenched dilution where the existence of a cluster of occupied sites that spans the whole lattice is required for the occurrence of an ordered phase. The situation of our model is different, however, since vacancies are not quenched and the fact that clusters of occupied sites are continuously changing in time is likely to affect the propagation of order more the higher concentration of these vacancies. One should stress again that this model is also different from a site annealed diluted Ising system; the dynamic rules for the present model do not lead to phase separation as occurs in the annealed Ising model with site dilution.

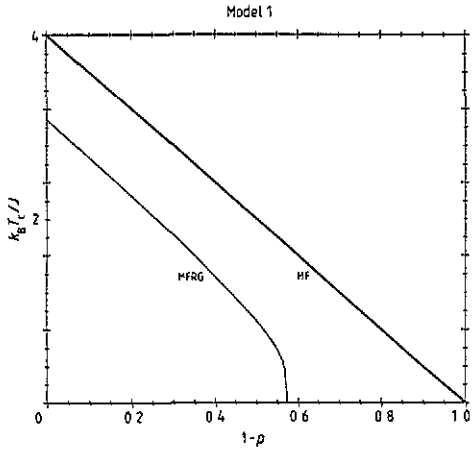

Figure 1. Plot of $1/K_c = k_B T_c/J$ as a function of p, as obtained by MFRG, for model 1. The critical line predicted by simple mean-field theory is indicated by MF.

In figure 1, we have also represented the critical line predicted by mean-field theory (obtained by equating $P(1) - P(-1)$ and m'). As found before with other systems [15], a simple MF theory is not capable of predicting the correct vanishing of T_c for a certain $q^* \neq 1$.

As will be shown in section 4, the phase diagram thus obtained by MFRG is in qualitative agreement with the results of computer simulations.

3.2. Model 2

The limit $p = 0$ of this model corresponds to the Ising case. Except for $p = 1$ (when all the states 1, 2 and 3 are equivalent—this is just the three-state Potts case), the competition with process D results in unequal treatment of state 1, similar to what happened to the state 0 (vacancy) in the previous model; one still expects symmetry breaking between states 2 and 3 to occur below a certain critical temperature $T_c(p)$ whereas the average number of sites in state 1 behaves as a non-ordering parameter.

The procedure for the implementation of MFRG method is, therefore, similar to the one sketched above, with the differences introduced by the new rates, which indeed lead to lengthier calculations; the result for $T_c(p)$ is shown in figure 2(a). The curve interpolates between approximate values for the critical temperature of the Ising and three-state Potts models; we have no explanation for the apparent plateau, it may just result from the approximation itself. In figure 2(b) we have plotted the p dependence of the non-ordering parameter Q along the transition line:

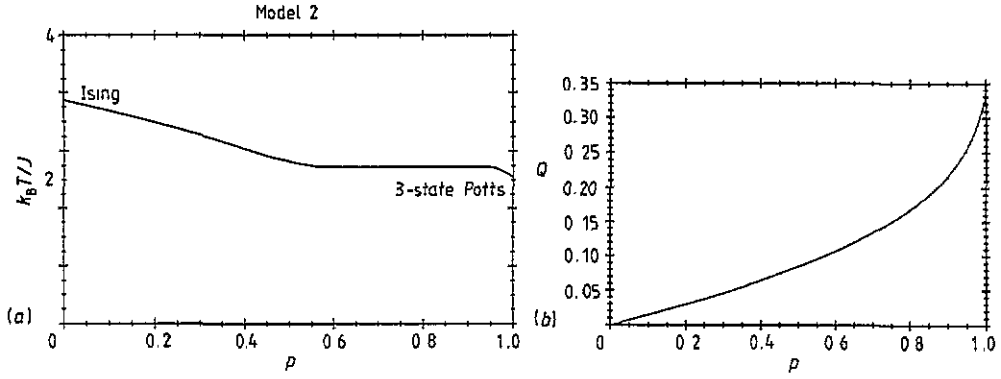

Figure 2. (*a*) Plot of k_BT_c/J as a function of p, as obtained by MFRG, for model 2. (*b*) p-dependence of the non-ordering parameter Q along the transition line, as given by MFRG, for model 2.

$Q = 0$ for the Ising case and $Q = \frac{1}{3}$ for the three-state Potts system at the transition point.

There is a quenched disordered equilibrium system whose phase diagram resembles this one [16]. In this model, some sites are occupied by Ising spins and others by Potts spins. The same comments we made above for the model with vacancies would apply here, and we do not believe an effective Hamiltonian can be found that describes this dynamic process.

4. Computer simulations

4.1. Model 1

We have simulated this model on a square lattice with $L \times L$ sites, L ranging from $L = 20$ to $L = 128$; we used periodic boundary conditions and random initial configurations. Starting with a given configuration, the following one was obtained by (i) choosing a site i at random; (ii) generating a random number s uniformly distributed in $[0,1]$; (iii) if $s > p$ then site i becomes vacant; otherwise: (1) generating another random number r; (2) if $r < \frac{1}{2}(1+\tanh x_i)$ then $S_i' = 1$; otherwise $S_i' = -1$. The first configurations were discarded as we were only interested in the stationary regime. We performed a variable number of Monte Carlo (MC) steps (one MC step corresponds to L^2 spin-flip attempts) according to the size of the lattice and to whether we wanted to span a large temperature range or just to obtain accurate values in a narrow region around $T_c(p)$: typical values ranged from 2×10^4 to 10^5 MC in the former case, and reached 5×10^6 MC in the latter.

The magnetization $M_L = \langle |m_L| \rangle$, where $m_L = \sum_i \sigma_i / L^2$, is shown in figure 3 as a function of the temperature for different values of p, and $L = 128$. The critical temperature is shown to decrease as p is lowered and the ordered state disappears for $p < p^*$. From looking at figure 3 we can guess that $p^* < 0.62$, but one has to consider corrections due to finite size effects; these are accounted for in the finite-size scaling analysis presented below in this section and shown to be consistent with $p^* = 0.620 \pm 0.002$.

In figure 4 we have plotted $T_c(p)$ as obtained from simulations. To locate the critical point at each value of p, we have considered [17] the point of intersection

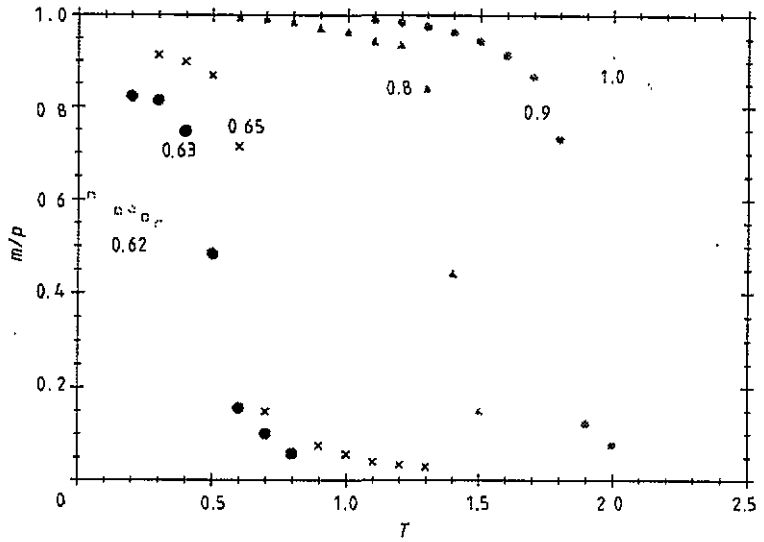

Figure 3. Model 1: the magnetization as a function of the temperature for different values of p, and $L = 128$. Data for $p \neq 1$ were obtained with 2×10^4 MC steps; points for $p = 1$, in the vicinity of the transition were obtained by performing 10^5 MC steps.

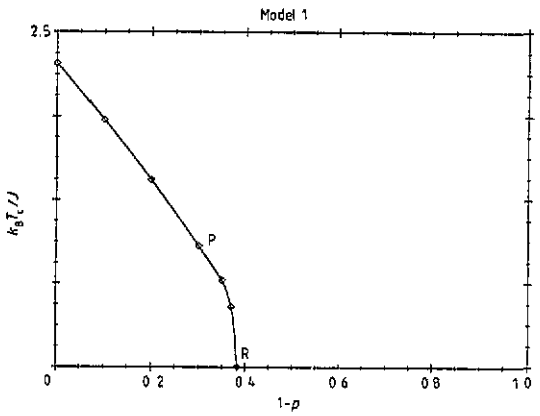

Figure 4. $T_c(p)$, for model 1, as obtained from simulations.

of the curves that represent the fourth-order cumulant $u_L = 1 - \langle m_L^4 \rangle / 3 \langle m_L^2 \rangle^2$ as a function of T, for different values of L. We have chosen to study more carefully two points along the critical line: point P, corresponding to $p = 0.7$; and point R, the transition point at $T = 0$. In what follows, we analyse the results of the simulations and the estimates obtained for the exponents that describe critical behaviour around these two points.

We start with the critical behaviour at $p = 0.7$. The estimate for the critical temperature $T_c = 0.905 \pm 0.01$ is obtained by three independent procedures:

(i) Figure 5(*a*) shows a plot of u_L as a function of T for different values of L. $u_L(T)$ scales like $u_L(T) = \tilde{u}(L^{1/\nu}\epsilon)$ [17,18] where ϵ is the reduced temperature, and therefore all curves for different L must intersect at a fixed value, u^*. We get $u^* = 0.605 \pm 0.06$ which is consistent [19] with the value obtained in two-dimensional systems belonging to the universality class of the Ising model.

(ii) In figure 5(*b*) we have represented T versus $(m^*)^{1/\beta}$, where m^* are

extrapolated values of the magnetization (using L^{-2} as the appropriate abscissa variable for such an extrapolation, under periodic boundary conditions [20]) and $\beta = \frac{1}{8}$, the Onsager value for the critical exponent β. The data give a reasonable fit to a straight line, thus supporting the idea that the critical behaviour is indeed Ising-like. The line intersects the vertical axis at a value of T consistent with the above estimate for T_c.

(iii) Finally, in figure 5(*c*) we have plotted T_L^*, the value of T for which the susceptibility $\chi_L = N\langle m_L^2\rangle - \langle|m_L|\rangle^2$ is at a maximum, as a function of $1/L$. From the scaling relation [18] $\chi_L(T) = L^{\gamma/\nu}\tilde{X}(L^{1/\nu}\epsilon)$ it follows that $T_L^* = T_c + x^*/L^{1/\nu}$; $\nu = 1$ for the Ising model, so a straight line is expected and T_c can be obtained from the intersection with the vertical axis. The data presented in figure 5(*c*) again fit into this picture and verify the estimate obtained above for the critical temperature.

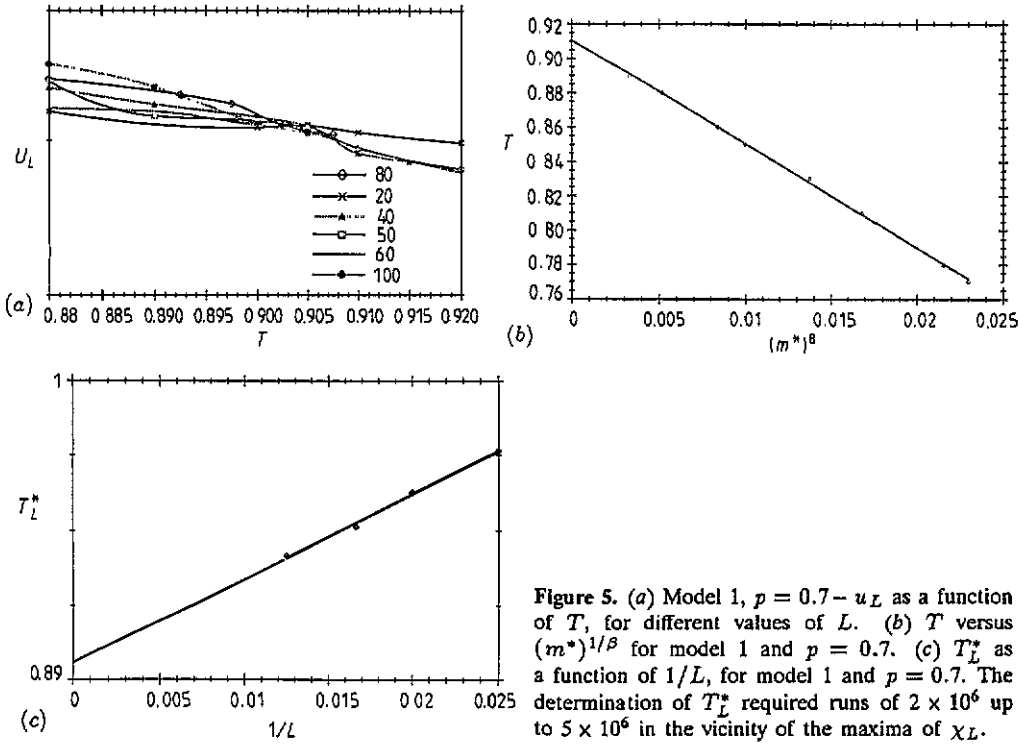

Figure 5. (*a*) Model 1, $p = 0.7 - u_L$ as a function of T, for different values of L. (*b*) T versus $(m^*)^{1/\beta}$ for model 1 and $p = 0.7$. (*c*) T_L^* as a function of $1/L$, for model 1 and $p = 0.7$. The determination of T_L^* required runs of 2×10^6 up to 5×10^6 in the vicinity of the maxima of χ_L.

To obtain an estimate of γ/ν and β/ν we calculated, for different lattice sizes, the magnetization and the susceptibility at $T_c = 0.904$. From the finite-size scaling relation for the susceptibility and the one for the magnetization [18] $M_L(T) = L^{-\beta/\nu}\tilde{M}(L^{1/\nu}\epsilon)$, one gets that $\chi_L(T_c) \propto L^{\gamma/\nu}$ and $M_L(T_c) \propto L^{-\beta/\nu}$, thus enabling one to obtain γ/ν and β/ν from the slopes of the log–log plots of $\chi_L(T_c)$ and $M_L(T_c)$ versus L. These are shown in figures 6(*a*) and 6(*b*), the best fit giving $\gamma/\nu = 1.71 \pm 0.05$ and $\beta/\nu = 0.125 \pm 0.005$. In figure 6(*a*) we also include another log–log plot of the maximum value of the susceptibility, χ_L^*, versus L; from the above, $\chi_L^* = L^{\gamma/\nu}\tilde{X}(x^*)$, so another estimate for γ/ν can be obtained in this way. The best fit gives $\gamma/\nu = 1.75 \pm 0.05$.

We refer now to the simulations for this system at $T = 0$. In this limit, the rates are very simple: the randomly chosen site becomes vacant with probability $1 - p$

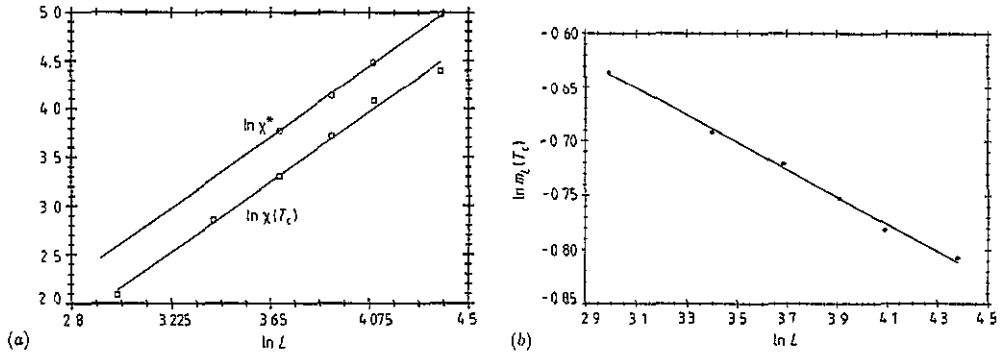

Figure 6. (*a*) Model 1, $p = 0.7-$ log–log plot of $\chi_L(T_c = 0.904)$ and $\chi_L^* = \chi(T_L^*)$ as a function of L. (*b*) Model 1, $p = 0.7-$ log–log plot of $M_L(T_c)$ versus L. Runs of 2×10^6 were used at T_c.

and adopts the majority sign of the spins in its neighbourhood with probability p, choosing either $+1$ or -1 with probability $p/2$ if the sum of the neighbours is zero. This is somewhat similar to what happens with the isotropic majority-vote model [19], where a phase transition to a disordered state results from the competition with a process where the site opposes the majority sign of its neighbours. In our case, this is achieved by the process of emptying a site, with probability $1 - p$.

We followed basically the same procedure as above, but for brevity we shall only refer to the most relevant results.

From the intersection of the $u_L(p)$ curves we arrived at $u^* = 0.611 \pm 0.003$, $p_c = 0.620 \pm 0.002$. Figures 7(*a*) and 7(*b*) are the equivalent of figures 6(*a*) and 6(*b*) for this case. One arrives at the following estimates: $\beta/\nu = 0.130 \pm 0.005$ and $\gamma/\nu = 1.74 \pm 0.03$. In fact, all the evidence obtained from the data seems to indicate that this critical point belongs to the universality class of the equilibrium Ising model. We have already stressed that despite a somewhat similar phase diagram, model 1 does not correspond to the quenched diluted Ising model. In that case, the critical exponents at $T = 0$, in the percolation limit, are, in fact, different from the ones predicted by Onsager for the Ising system. Also, p_c is, for model 1, slightly above the critical concentration for site percolation $p_c^{sp} = 0.59$ [21]; this means that continuous mobility of the clusters of occupied sites makes the propagation of order more difficult and may even prevent an ordered state at a narrow concentration range where it would still persist were these clusters quenched.

Having carefully analysed the critical behaviour at two representative points (P and R) of the phase diagram, we think that there is clear evidence of Ising-like critical behaviour all along the critical line shown in figure 4.

4.2. Model 2

We have performed computer simulations of this model following a procedure very similar to the one used in the study of model 1. After each MC step, the number $n_i(L)$ of sites in state i was recorded. For different values of p, and different system sizes, we measured $M_L = \langle |m_L| \rangle = 1/L^2 \langle |n_2(L) - n_3(L)| \rangle$ and $Q_L = 1/L^2 \langle n_1 \rangle$, as well as χ_L and u_L.

In figure 8(*a*) we have plotted $T_c(p)$ as obtained by analysis of the simulation data for u_L at different values of the parameter p. $p = 0$ and $p = 1$ correspond,

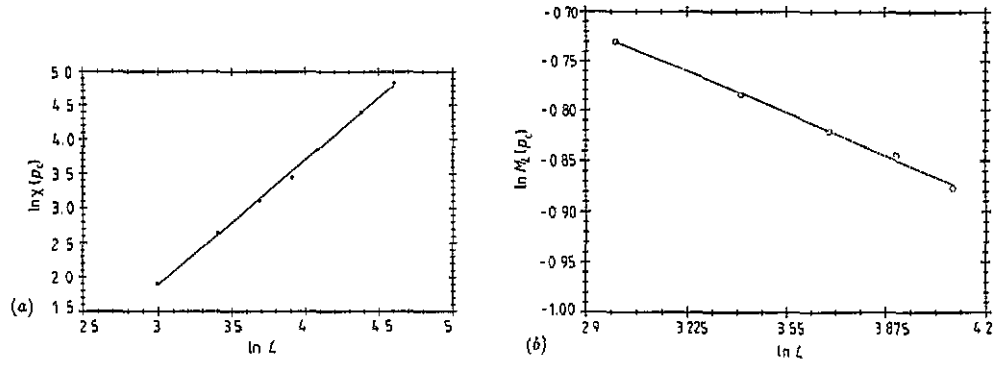

Figure 7. (*a*) Model 1, $T = 0-$ Log–log plot of $\chi_L(p_c = 0.620)$ as a function of L. (*b*) Model 1, $T = 0-$ Log–log plot of $M_L(p_c)$ versus L.

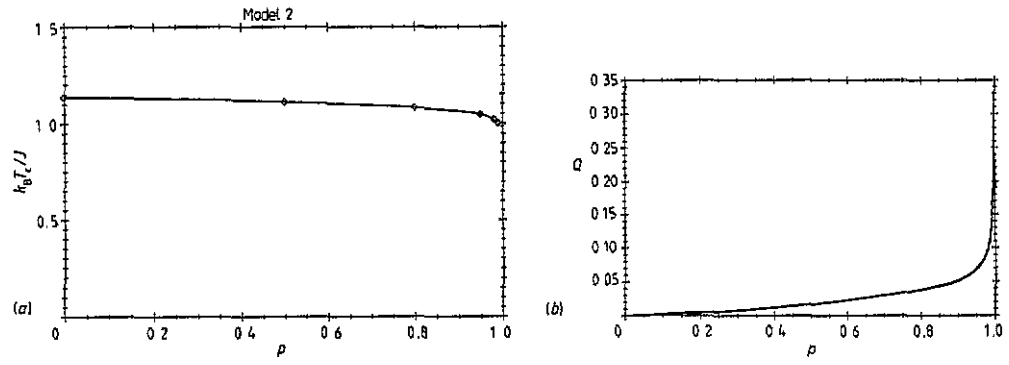

Figure 8. (*a*) $T_c(p)$, for model 2, as obtained from simulations. (*b*) $Q(p)$ along the critical line, as obtained by simulations, for model 2.

respectively, to the equilibrium Ising and three-state Potts systems and for these we have represented the exact results [22]. (In fact the symmetry breaking implied in our definition of M_L does not apply when $p = 1$, that is when there is no asymmetry in the space of Potts states.) As can be seen, the critical curve interpolates smoothly between these two critical points. In figure 8(*b*) we have included a plot of the values taken by the non-ordering parameter Q along the critical line. If one compares this with the one obtained by MFRG (figure 2(*b*)), one notices that $Q^{(\text{simulations})}$ is considerably lower than $Q^{(\text{MFRG})}$; this means that the presence of state 1 is not very significant in the vicinity of the phase transition, when symmetry breaking between states 2 and 3 occurs. The way $Q^{(\text{simulations})}$ approaches $\frac{1}{3}$ as $p \to 1$ is here seen to be very abrupt. We have no sensible explanation for this fact.

We have studied the critical behaviour in two points of the phase diagram: $p = 0.5$ and $p = 0.95$. Again strong evidence of Ising critical behaviour was found. Figure 9 and the estimates $\gamma/\nu = 1.72 \pm 0.03$ and $\beta/\nu = 0.129 \pm 0.05$ illustrate this point. The value of u^* found for different values of p was again consistent with the values it takes at the Ising critical point. We therefore conclude that the critical behaviour displayed by model 2 is Ising-like all along the critical line and only the point at $p = 1$ corresponds to a different critical behaviour (three-state Potts). If it is legitimate to

use the language of RG, one would say that the three-state Potts fixed point is unstable to the inclusion (via dynamics) of any anisotropy in the space of Potts states.

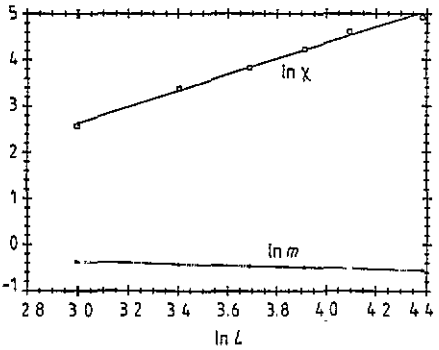

Figure 9. Model 2, $p = 0.5$– log–log plot of $\chi_L(T_c = 1.109)$ and $M_L(T_c)$ versus L.

5. Conclusion

The phase diagram of two different non-equilibrium three-state systems, in two dimensions, is here studied by means of an analytical method (MFRG) and computer simulations; there is qualitative agreement between the results of both approaches. A finite-size scaling analysis of the MC data led to estimates for the critical exponents, all consistent with the values for the equilibrium Ising model, thus confirming the symmetry analysis of Grinstein *et al* [9]. As a matter of fact their study concentrates on two-state dynamic systems but the argument that the presence of up–down symmetry leads to Ising critical behaviour is actually expressed in terms of a continuum Langevin equation; a coarse-grained version of the Langevin equation for the present three-state models (both having the up–down symmetry of the Ising model) should therefore be of the same form (at large enough distances) and thus lead to the same universality class.

Further investigation of other three-state (or arbitrary number of states) non-equilibrium systems with or without this symmetry is still needed for a complete test of the above argument.

Acknowledgments

I would like to thank M Droz for his hospitality and advice at the University of Geneva where the numerical part of this work was started. Many thanks also to J F Mendes for his help with computer work, and to M de Oliveira, M A Santos and T Tomé for very useful discussions. This work was partially supported by JNICT, project CEN-386/90.

References

[1] Haken H 1983 *Synergetics* (New York: Springer)
[2] Nicolis G and Prigogine 1977 *Self-Organization in Nonequilibrium Systems* (New York: Wiley)

[3] López-Lacomba A I, Garrido P L and Marro J 1990 *J. Phys. A: Math. Gen.* **23** 3809
[4] Dickman R 1989 *Phys. Rev.* B **40** 7005
[5] Wang J S and Lebowitz J L 1988 *J. Stat. Phys.* **51** 893
[6] Garrido P L, Labarta A and Marro J 1987 *J. Stat. Phys.* **49** 551
[7] Marques M C 1990 *Phys. Lett.* **145A** 379
[8] Marques M C 1989 *J. Phys. A: Math. Gen.* **22** 4493
[9] Grinstein G, Jayaprakash C and He Y 1985 *Phys. Rev. Lett.* **55** 2527
[10] Ziff R M, Gulari E and Bershad Y 1986 *Phys. Rev. Lett.* **56** 2553
[11] Kinzel W 1985 *Z. Phys.* B **58** 229
[12] Cornell S, Droz M, Dickman R and Marques M C 1991 *J. Phys. A: Math. Gen.* **24** 5605
[13] Mendes J F to be published
[14] Marques M C 1990 *Physica* A **163** 915
[15] Kaneyoshi T and Mielnicki J 1990 *J. Phys.: Condens. Matter* **2** 8773
[16] Marques M C, Santos M A and Oliveira J M B 1987 *J. Phys. A: Math. Gen.* **20** 5701
[17] Binder K and Heermann D W 1988 *Monte Carlo Simulations in Statistical Physics* (Berlin: Springer)
[18] Privman V 1990 *Finite-size Scaling and Numerical Simulation of Statistical Systems* (Singapore: World Scientific)
[19] de Oliveira M J 1992 *J. Stat. Phys.* **66** 273
[20] Binder K 1979 *Monte Carlo Methods in Statistical Physics* (Berlin: Springer)
[21] Stinchcombe R 1983 *Phase Transitions and Critical Phenomena* vol 7, ed C Domb and J L Lebowitz (New York: Academic) pp 152–280
[22] Wu F Y 1982 *Rev. Mod. Phys.* **54** 23